

Control of myocyte remodeling in vitro with engineered substrates

Nicholas A. Geisse · Sean P. Sheehy · Kevin Kit Parker

Received: 11 October 2008 / Accepted: 5 January 2009 / Published online: 28 February 2009 / Editor: J. Denry Sato
© The Society for In Vitro Biology 2009

Abstract Tissue microenvironments can regulate cell behavior by imposing physical restrictions on their geometry and size. An example of these phenomena is cardiac morphogenesis, where morphometric changes in the heart are concurrent with changes in the size, shape, and cytoskeleton of ventricular myocytes. In this study, we asked how myocytes adapt their size, shape, and intracellular architecture when spatially confined in vitro. To answer this question, we used microcontact printing to physically constrain neonatal rat ventricular myocytes on fibronectin islands in culture. The myocytes spread and assumed the shape of the islands and reorganized their cytoskeleton in response to the geometric cues in the extracellular matrix. Cytoskeletal architecture is variable, where myocytes cultured on rectangular islands of lower aspect ratios (length to width ratio) were observed to assemble a multiaxial myofibrillar arrangement; myocytes cultured on rectangles of aspect ratios approaching those observed in vivo had a uniaxial orientation of their myofibrils. Using confocal and atomic force microscopy, we made precise measurements of myocyte volume over a range of cell shapes with approximately equal surface areas. When myocytes are cultured on islands of variable shape but the same surface area, their size is conserved despite the changes in cytoskeletal architecture. Our data suggest that the internal cytoskeletal architecture of the cell is dependent on extracellular boundary conditions while overall cell size is not, suggesting a growth control mechanism independent of the cytoskeleton and cell geometry.

Keywords Microcontact printing · Cytoskeleton · Myofibril · Cardiac myocyte · Atomic force microscopy · Confocal microscopy

Introduction

Cell shape and the cytoskeleton regulate many cellular processes and play an important role in migration, cell cycle control, proliferation, and apoptosis (Chen et al. 1997; Huang et al. 1998; Parker et al. 2002; LeDuc and Bellin 2006). Cell shape in the heart may also be associated with cardiomyopathies, where distinct relationships between the shape of ventricular myocytes and contractile function have been reported by Gerdes and colleagues (Gerdes and Capasso 1995; reviewed in Gerdes 2002). Commonly, myocyte shape and size serve as quantitative metrics in assays of myocyte hypertrophy and viability in vitro. Unfortunately, in typical culture conditions, myocytes lose their characteristic morphology with time, becoming pleomorphic with isotropic cytoskeletal architecture. New culture techniques, however, based on soft lithography are capable of controlling myocyte shape and preserving the length to width ratios (Parker et al. 2008; Bray et al. 2008) observed by Gerdes and colleagues.

In this study, we asked whether the size and cytoskeletal architecture of cardiac myocytes changes with shape. Using microcontact printing, we have engineered neonatal rat ventricular myocytes by culturing them on islands of varying length to width proportions (aspect ratios) with a constant cell-substrate contact area. Using atomic force microscopy (AFM), high resolution, three-dimensional topographical maps of living cardiac myocytes were collected and their volumes were measured. High resolution confocal microscopy stacks confirm this topography, where

N. A. Geisse · S. P. Sheehy · K. K. Parker (✉)
School of Engineering and Applied Sciences, Harvard University,
29 Oxford Street, Pierce Hall 322a,
Cambridge, MA 02138, USA
e-mail: kkparker@seas.harvard.edu

myofibrils are constrained to the cell–substrate interface with the nucleus above the myofibrillar array. Furthermore, our results show that myofibrillar architecture is a predictable function of the geometric cues in the extracellular matrix (ECM). These results are important, because they suggest that myocytes have unique responses to in vitro culture conditions that should be considered, and controlled, in the design of experimental protocols.

Material and Methods

Cell culture. All procedures described below were conducted according to the guidelines of the Harvard University Animal Care and Use Committee. Ventricular myocytes were isolated from 2-d-old Sprague Dawley rats as briefly described. Excised ventricular tissue was agitated in a 0.1% trypsin solution cooled to 4°C for approximately 14 h. Trypsinized ventricles were dissociated into their cellular constituents via serial exposure to a 0.1% solution of collagenase type II at 37°C for 2 min. The myocyte portion of the cell population was enriched by passing the dissociated cell solution through a nylon mesh with 40 µm pores and then pre-plating twice for 45 min each time. Isolated myocytes were seeded onto coverslips with patterned fibronectin substrates in culture medium consisting of 10% FBS. On the second day of culture, the serum concentration of the medium was reduced to 2% and the medium was changed every 48 h that the myocytes were kept in culture.

Microcontact printing. Micropatterning of myocytes was adapted from a technique developed previously by Tan and colleagues (Tan et al. 2004). Briefly, masks were designed in AutoCAD LT (Autodesk Inc., San Rafael, CA) and fabricated on a DWL66 direct write pattern generator (Heidelberg Instruments, Heidelberg, Germany). Silicon wafers (Wafer World, W. Palm Beach, FL) were spun coat with SU-8 2 photoresist (MicroChem Corp, Newton, MA) to a height of 2.5–3.0 µm. The mask was placed on the silicon wafer and exposed to UV light for 5 s using a Mask Aligner (Suss MicroTec, Waterbury, VT). Substrates were developed in propylene glycol monomethyl ether acetate, rinsed in isopropanol, and silanized overnight under vacuum. Once silanized, uncured polydimethyl siloxane (PDMS) was poured onto the wafer and cured at 70°C for 4 h. Stamps were cut from the wafer and cleaned with bath sonication in a 50/50 mixture of ethanol and water, and then ‘inked’ with a 50 µg/mL solution of fibronectin (FN) for 1 h at room temperature (RT). Coverslips that had been spincoated with a thin layer of PDMS were treated in a model 342 UV-ozone cleaner (Jelight Company, Inc., Irvine, CA) to oxidize the PDMS layer and were used

immediately for stamping. Fibronectin-coated stamps were placed onto coverslips for 5 min and were then blocked in 1% F127 Pluronic Acid (BASF, Mount Olive, NJ) for 5 min. Coverslips were rinsed in phosphate-buffered saline (PBS) before myocyte plating.

Immunofluorescence and confocal imaging. Cardiac myocytes were fixed 72 h after plating. Medium was removed by rinsing the cells in 37°C PBS and myocytes were immediately fixed in a 4% solution of paraformaldehyde with 0.01% Triton X-100 in phosphate-buffered saline at 37°C. During the 15 min fixation period, myocytes were equilibrated to room temperature. After fixation, myocytes were rinsed in PBS at RT and stained. Myocytes were stained by inverting the coverslip on a solution of PBS containing 4',6'-diamidino-2-phenylindole hydrochloride (DAPI, 30 nM) and alexa-fluor 488-conjugated phalloidin (0.2 U) (all available from Invitrogen, Eugene, OR). The first stain also contained a 1:200 dilution of anti-sarcomeric α -actinin monoclonal antibody (clone EA-53, Sigma, St. Louis, MO) and was incubated for 1 h at RT. Before the secondary stain, coverslips were rinsed three times in RT-PBS. Secondary stains contained a 1:200 dilution of tetramethyl rhodamine-labeled goat anti-mouse IgG (H+L chain) antibody (Invitrogen). After incubation, coverslips were again rinsed and mounted in a DABCO-based preservative until imaged.

Confocal microscopy was performed on a Zeiss LSM LIVE laser line scanning confocal microscope (Carl Zeiss, Jena, Germany). Samples were imaged with a 63X plan-apochromatic NA 1.4 objective. Optical Z sections were taken every 0.25 µm and data were analyzed and displayed using ImageJ (NIH, Bethesda, MD). Confocal images are displayed as single-plane (substrate surface) xy images or as zx stack projections.

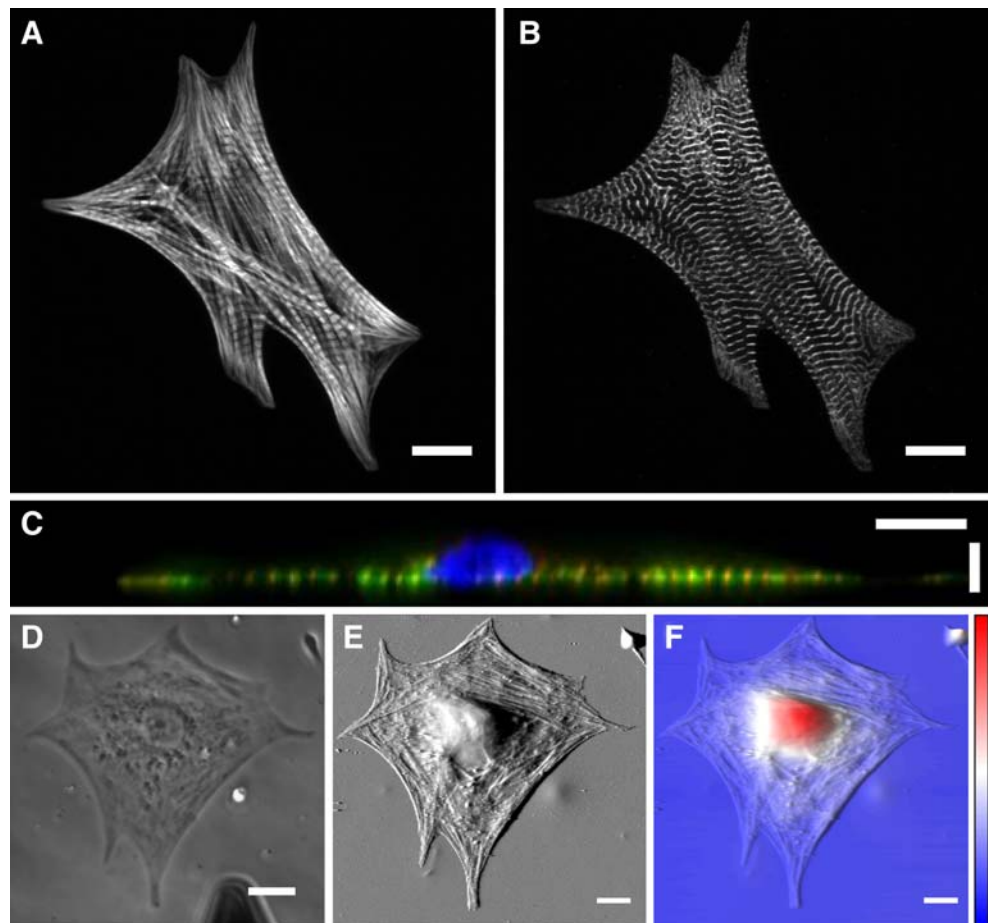
Atomic force microscopy (AFM). Atomic force microscopy was carried out with an MFP-3D-IO AFM (Asylum Research, Santa Barbara, CA) mounted on a Zeiss Axiovert 200 MAT. Myocytes were imaged in Normal Tyrode's solution (135 mmol/L NaCl, 5.4 mmol/L KCl, 1.0 mmol/L MgCl₂, 1.8 mmol/L CaCl₂, 5.0 mmol/L HEPES, 5.0 mmol/L Glucose, 0.33 mmol/L NaH₂PO₄, pH=7.4) and were identified by 40X phase contrast imaging. Mononucleated cardiac myocytes that were actively contracting were selected for imaging. Silicon nitride probes with nominal spring constants of 0.01 N/m (Veeco Probes, Santa Barbara, CA) were used and contact mode imaging force was chosen to maximize signal to noise ratio and ensure that trace and retrace images were identical. All probes were calibrated utilizing the thermal tune method (Walters et al. 1996) in order to account for deviations of the nominal spring constants due to manufacturing fidelity. AFM images were

modified by the application of a 0th order flatten and no other data modification or transformations were performed. Volume was calculated by selecting a threshold in which all parts of the scan that were above the substrate level were contained and by applying volume calculation software (Asylum Research) in the IgorPRO programming environment (Wavemetrics, Lake Oswego, OR) and are reported as μm^3 . In order to accommodate small deviations in pattern and myocyte size, myocyte size measurements were normalized by dividing volume by apical surface area ($\text{fL}/\mu\text{m}^2$) as measured by the image processing threshold. All measured volume/area values were compared across types using the Wilcoxon–Mann–Whitney two sample rank test (Glantz 2002). Threshold for rejection of the null hypothesis was $p < 0.05$. When the average volume measurements for each cell type was compared to the average volume of every other cell type, in each case the two sample rank test reported p values > 0.05 , therefore no difference between data sets could be detected using this statistical test, indicating that the volumes across cell types were statistically similar.

Results

The myocyte cytoskeleton is organized with respect to geometric cues in the ECM. When ventricular myocytes are chemically dissociated from the ventricles of neonatal rats, they are cylindrical in shape. However, they change their shape after 24–48 h in culture on unbounded stiff silicone substrates coated with FN protein (Fig. 1). Pleomorphic myocytes generally displayed isotropic sarcomere alignment until the length to width ratio exceeded unity. When this occurs, myofibrils tend to align and there appears to be lateral coupling of adjacent myofibrils at the sarcomere Z-lines, an example of which is shown in Fig. 1A–B. In these cells, the emergent anisotropy suggests a polarization of the contractile apparatus. Confocal microscopy reveals that the myofibril array were organized primarily at the cell–substrate interface and cross-sectional imaging in z reveals that the nucleus generally rests on top of the myofibrillar layer (Fig. 1C). Using an AFM in contact mode, the apical surface of cultured myocytes was mapped, and when these measurements of the height profile are taken together with

Figure 1. Confocal slices of fixed myocytes fluorescently labeled for actin (A) and α -actinin (B), and the Z-stack projection profile (C), show the gross 3D morphology of fixed myocytes in culture. Simultaneous phase contrast (D) and AFM deflection (E) and pseudo color 3D projection of height (F) of pleomorphic myocytes show the same morphology for live cells. Horizontal scale bars = 10 μm , vertical scale bar = 5 μm , color scale for (F) = 4 μm blue to red.

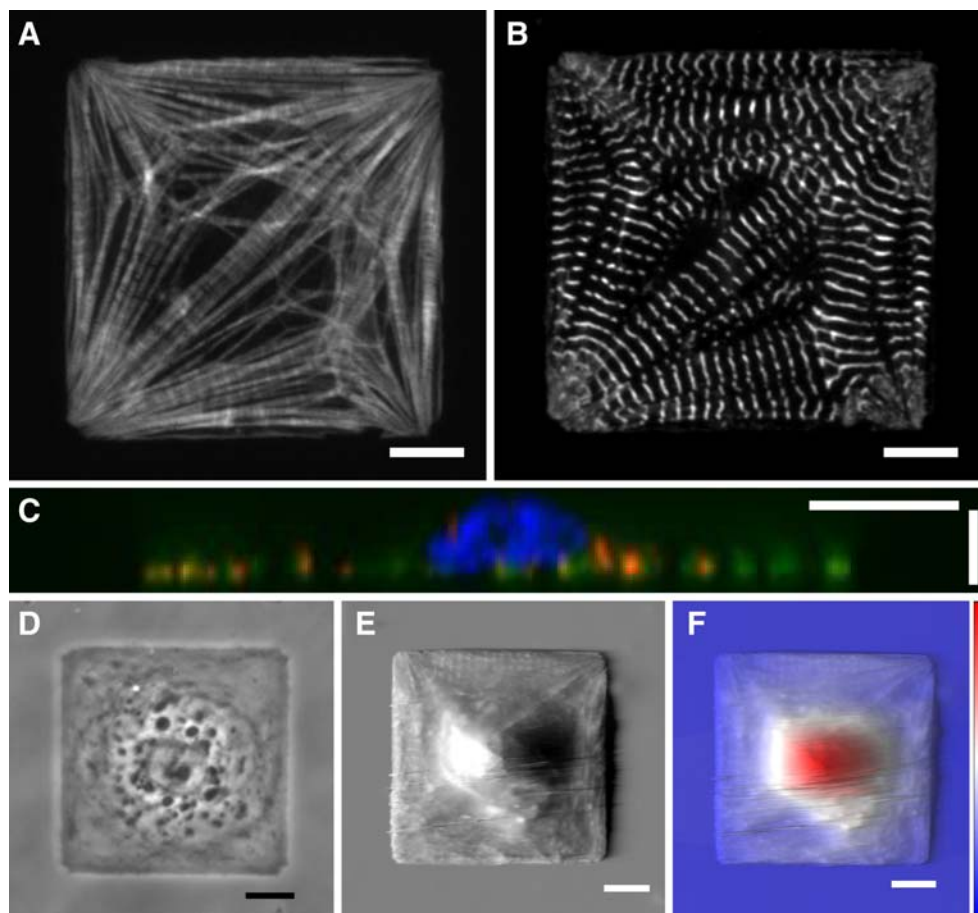


confocal stacks, it confirms that the contractile cytoskeleton is constrained to a layer above the cell–substrate interface (Fig. 1E and F). In these experiments, live pleomorphic myocytes were identified optically with phase contrast microscopy and those which were beating were scanned with the AFM mounted on an inverted optical microscope (Fig. 1D). The deflection of the AFM cantilever at a given point in the xy plane is measured in order to resolve the myocyte topography and membrane–substrate edges (Fig. 1E). The displacement of the z -piezo is mapped in the xy plane, yielding a map of the myocyte height (Fig. 1F). These data from the control experiments suggest what is widely known, namely, that the morphology of myocytes in vitro varies significantly from that in vivo and may suggest their unsuitability as a valid model of in vivo cell physiology.

To better approximate their native cytoskeletal architectures, cells can be cultured on constraining substrates in vitro that mimic their in vivo morphologies. In this study, this was accomplished by culturing the myocytes on islands of FN with specific sizes and geometries micropatterned onto stiff silicone substrates. Myocytes spread and remodeled to assume the shape of the patterned island over the course of 24–48 h

after plating. Much like myocytes that were cultured without 2D boundary conditions, myocytes patterned onto $50 \times 50 \mu\text{m}$ ($2,500 \mu\text{m}^2$) squares also assumed a myofibrillar structure that was primarily in a 2D layer adjacent to the myocyte–substrate interface, although in this case myofibrils were aligned along the diagonals and boundary edges of the myocyte repeatedly, as shown in the examples in Fig. 2A–B. Like the pleomorphic myocytes, the nucleus in these square myocytes is generally positioned above the myofibrillar array at the cell–substrate interface (xy plane) (Fig. 2C). Beating, square myocytes identified by phase contrast optical microscopy (Fig. 2D) were scanned with the AFM in contact mode to examine the deflection and height profiles of the apical membrane (Fig. 2E–F). Like pleomorphic myocytes, AFM height images of engineered myocytes show that the bulk of the cytoplasm is within microns of the substrate surface, while the nucleus protrudes upward 2–3 μm in z (Fig. 2F). The repeatability of the myofibril and actin alignment in square myocytes over hundreds of immunostained coverslips suggest that the myofibril alignment can be precisely guided by geometric constraint of the myocyte in vitro and suggest a method of better replicating the aspect ratios of myocytes in adult hearts.

Figure 2. Confocal microscopy of fluorescently labeled actin (A) and α -actinin (B) and the Z -stack projection profile (C) of a micropatterned myocyte reveal similar organization to pleomorphic cells in Fig. 1. A living myocyte chosen by phase contrast microscopy (D) shows similar morphology in the deflection (E) and pseudo color 3D height projection (F). Horizontal scale bars = 10 μm , vertical scale bar = 5 μm , color scale for (F) = 4 μm blue to red.



To test this idea, we decided to engineer myocytes with a broader range of aspect ratios while attempting to hold the area of the myocytes approximately constant. Similar morphologies were evident in myocytes cultured on patterned rectangles with increasing ARs (Fig. 3) when analyzed by confocal microscopy (Fig. 3A–C). When a single myocyte occupies a FN island, they spread and uniformly cover the island surface, assuming the shape of the island. Unlike other cell types, myocytes do not extend lamellipodia from the island boundaries. As shown in the example images of Fig. 3A and B, as the AR of the myocytes is increased, the alignment of the myofibrils along the myocyte diagonal falls away until a uniformly anisotropic myofibrillar array appears parallel to the longitudinal axis of the rectangular myocytes. This contractile architecture suggests that as the constrained myocytes have their AR increased, a polarity that merges that

affords the myocyte a uniform and directed contraction. As for the previous studies, we first identified beating, mononucleated myocytes on island shapes of interest by phase contrast microscopy (Fig. 3D). Immunostaining and AFM (Fig. 3E) data suggest that the nucleus preferentially localizes to the center of the myocyte, while AFM height images of patterned cells (Fig. 3F) suggest that in these experimental conditions, the nucleus is about the same size.

Two-dimensional alignment of the sarcomeres in patterned myocytes shows trends based on extracellular boundary conditions. When myocytes are cultured on longer and narrower aspect islands (i.e., 5:1 and 7:1), of actin stains (Fig. 3A) and sarcomeric α -actinin stains (Fig. 3B) reveal that myofibrils generally align with the long axis of the myocyte. However, at smaller aspect ratios, such as 1:1, 2:1, and 3:1, Z-line staining suggests that myofibrils align perpendicularly to both the short and long

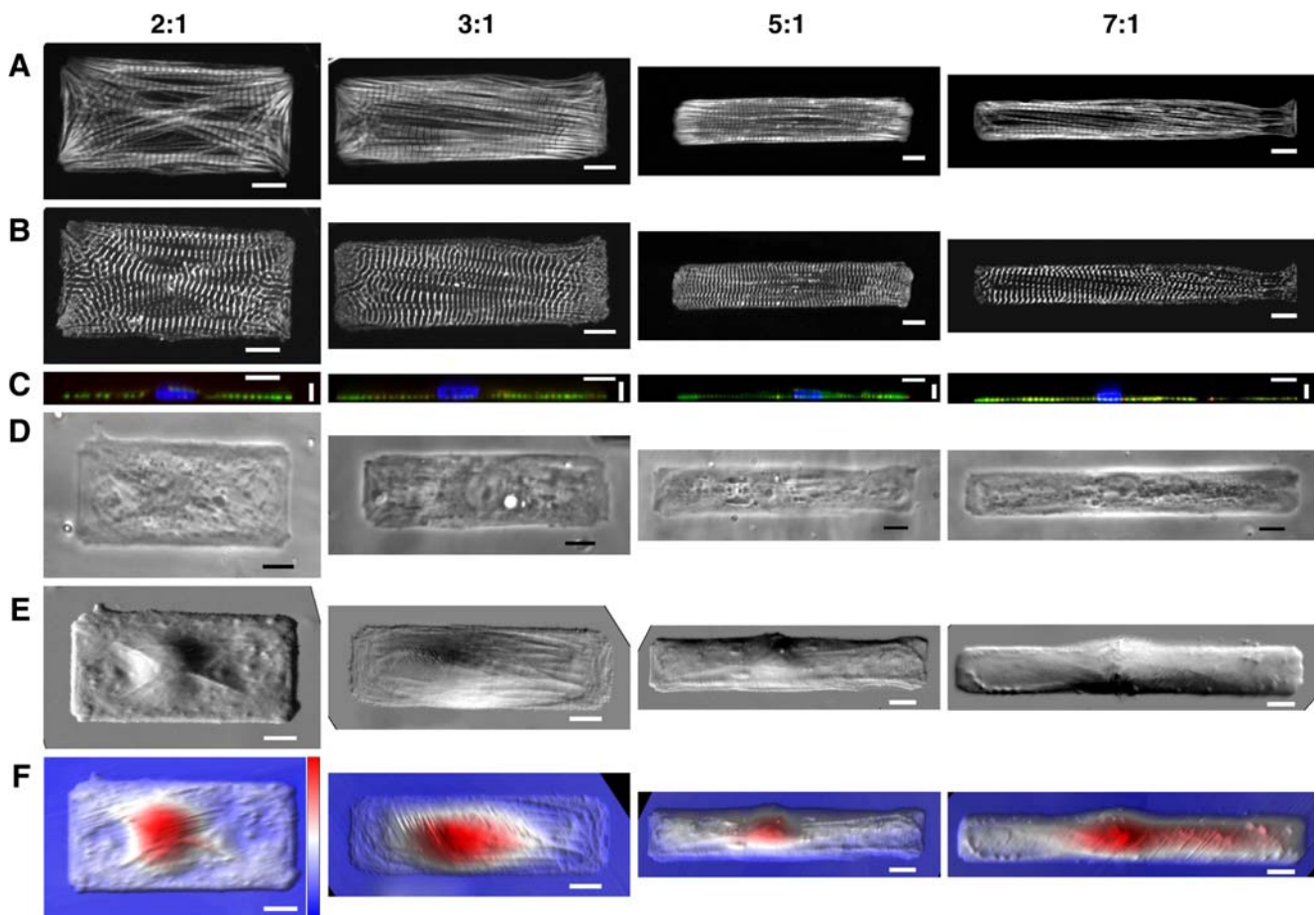
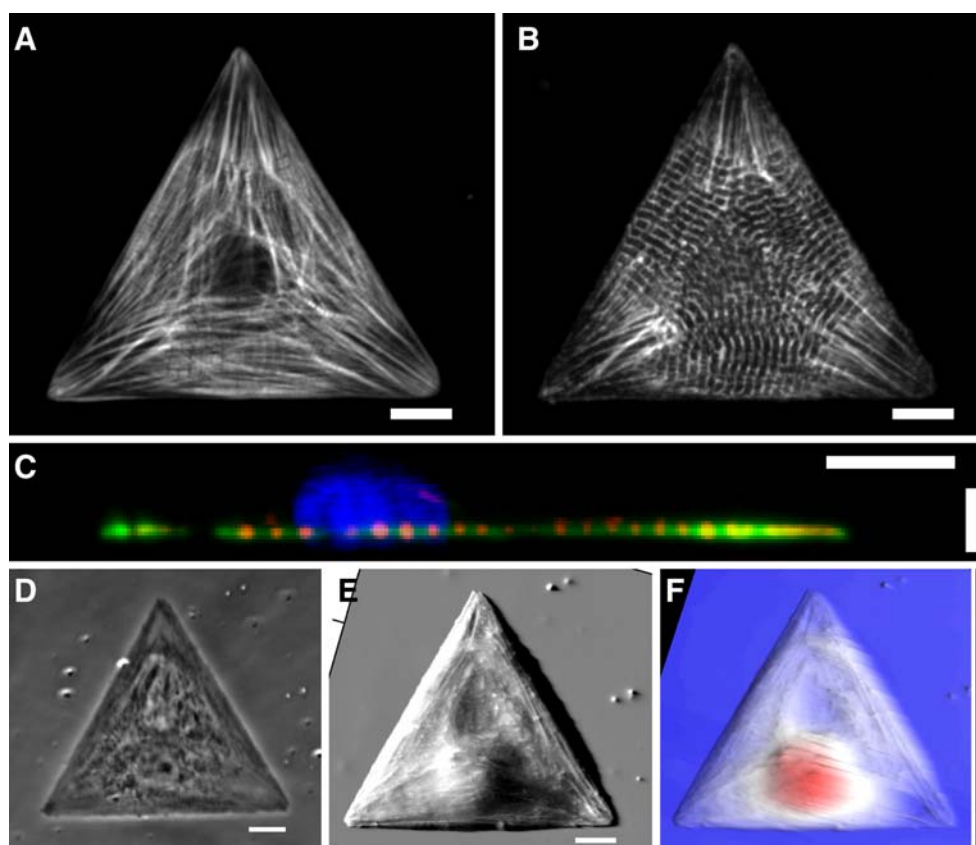


Figure 3. Isolated confocal slices of myocytes patterned on rectangular FN islands at various aspect ratios (columns 2:1, 3:1, 5:1, and 7:1, approximately) show the 2D morphology of the myofibrils in the myocyte–substrate interface plane with respect to actin (row A) and α -actinin (row B). Image processing and profile projection of confocal microscopy data from fixed cells (row C) demonstrates that the nucleus (blue) sits on top of the myofibrillar architecture (green, actin;

red, α -actinin). Live myocytes identified with phase contrast microscopy (row D) were scanned with AFM (row E–F deflection and 3D pseudocolored projection, respectively). Horizontal scale bars = 10 μ m, vertical scale bar = 5 μ m, color scale for (F) = 4 μ m blue to red. AFM images for 5:1 and 7:1 myocytes were made from composites of two subsequent scans of the same cell.

Figure 4. Micropatterned myocytes on triangular ECM islands show a triaxial alignment of myofibrils as revealed by fluorescence microscopy of actin (A) and sarcomeric α -actinin stains (B). XZ projections of the confocal stack show that these myocytes adopt a similar, pseudo 2D arrangement of the nucleus and myofibrils (C). Phase contrast identification (D) of living myocytes scanned by AFM (E–F deflection and 3D pseudocolored projection) show similar architecture. Horizontal scale bars=10 μm , vertical scale bar=5 μm , color scale for (F)=4 μm blue to red.



axes of the 2:1 and 3:1 myocytes (Fig. 3A–B) while they are distributed symmetrically along the axes of the 1:1 cell (Fig. 2A–B) and are parallel to these edges.

We compared these results to triangular myocytes (Fig. 4). Actin (Fig. 4A) and α -actinin (Fig. 4B) stains in these myocytes show that myofibrils align along the long axes of the extracellular boundary, resulting in a tri-axial myofibrillar architecture. The nuclei of these myocytes are usually located at the center of the cell, as in all of the patterned myocytes. Myofibrils are located primarily below the nucleus coplanar with the substrate surface, as observed in rectangular myocytes (Fig. 4C). The apical surface of the triangular myocytes (Fig. 4D) appeared similar to the apical surface of the pleomorphic and rectangular myocytes, as indicated by AFM scans taken on a live myocyte (Fig. 4E–F).

Volume and area analyses were also performed on myocytes cultured onto rectangles of various aspect ratios and those data are summarized in Table 1. In order to measure the volume of cells in culture, AFM was used to obtain high-resolution topographical images of living cardiac myocytes in culture. Variations in the area are due to changes in the size of the micropatterned island, a direct result of the tolerances in the soft lithographic manufacturing process of the PDMS stamp. As can be seen from the data, the ratio of the myocyte volume to the surface area in the substrate plane is very similar, suggesting that in vitro, the mononucleated cell volume is conserved as a function

of the constraintment on the culture surface. When taken with the confocal images, these data suggest that in the island sizes used in this study, myofibrillogenesis can be roughly constrained in the plane of the substrate and that the nucleus is the primary contributor to the 3D volume. Thus, in studies of myofibrillogenesis, simplified experimental systems composed muscle cells cultured on precisely designed ECM islands can simply the 3D geometry of a myocyte in vivo to an experimental preparation that is amenable to multimodal microscopy and computer modeling studies.

Table 1. Cell area, volume, and volume/area of micropatterned NNRVMs across different aspect ratios and graph of the volume/area values

Cell type	Number	Area, $\mu\text{m}^2 \pm \text{SD}$	Volume μm^3 (fL) $\pm \text{SD}$	Vol/area $\pm \text{SD}$
Pleo	4	2,751 \pm 169	1,875 \pm 430	0.704 \pm 0.16
Tri	3	2,038 \pm 182	1,695 \pm 449	0.826 \pm 0.18
1:1	3	2,229 \pm 95	1,949 \pm 151	0.877 \pm 0.10
2:1	3	2,512 \pm 322	2,356 \pm 190	0.942 \pm 0.05
3:1	3	2,203 \pm 0.2	2,047 \pm 160	0.931 \pm 0.09
5:1	3	2,187 \pm 448	1,570 \pm 186	0.738 \pm 0.18
7:1	3	2,465 \pm 138	2,418 \pm 351	0.986 \pm 0.18

All values are presented as mean \pm Standard deviation

Discussion

Heart disease is often characterized by maladaptive remodeling of the muscular walls concurrent with fibrosis. On the cellular scale, individual myocytes also change and this is outwardly seen as changes in shape and increases or decreases in length-to-width or aspect ratio depending on the type of cardiomyopathy (Gerdes and Capasso 1995; Onodera et al. 1998; Gerdes 2002; Lammerding et al. 2004). In this study, we have used variable ECM templates to measure the ability of cardiac myocytes to remodel in vitro. Traditional studies of cardiac cell biology make use of freshly isolated myocytes, or myocytes that become pleomorphic over time in culture. This remodeling in vitro may bias results in studies of the fundamental mechanisms of cardiomyopathies because they fail to replicate the in vivo microenvironment. With these methods, measured cell volume is in the order of 20,000–37,000 μm^3 (Campbell et al. 1987; Delbridge et al. 1997) with typical cross-sectional areas of 190–240 μm^2 (Onodera et al. 1998) and these values greatly increase during hypertrophy. Data from our in vitro study indicates that changes in myocyte shape result in myofibrillar remodeling without significant changes in volume. Myofibrils in myocytes that were patterned into rectangles with 7:1 or 5:1 aspect ratios have an architecture that resembles that in the adult phenotype, where sarcomeres are perpendicular to the long (contractile) axis of the cell and actin filaments are longitudinal to the same axis. However, sarcomere alignment becomes bi-axial in 3:1 and 2:1 cells, with sarcomeric Z-lines perpendicular to both the long and short axes. In the case of square myocytes, sarcomere alignment is symmetrical along both axes in the xy plane of the cell, as sarcomeres are perpendicular to both xy boundaries and radiate out from the corners of these cells. This pattern of myofibrillar alignment is most evident in the case of the triangular cell, where the extracellular boundary conditions result in a triaxial cytoskeletal architecture. Further studies will reveal if these boundary conditions would potentiate changes in calcium handling or contractility, both of which are found to be altered in the diseased myocardium (Shorofsky et al. 1999; Lindner et al. 2002a, b).

Previously it has been reported that the cell-surface contact area can alter cell fates and gene transcription pathways, resulting in such diverse processes from proliferation to apoptosis (Chen et al. 1997), as well as alter the progression of the cell cycle (Huang et al. 1998). In our experimental system, varying the aspect ratio, but not the cell–substrate contact area, changes the myofibrillar architecture as measured by sarcomere alignment but cell volume remains constant. These results show that regardless of extracellular boundary conditions, cardiac myocytes cell size (as measured by volume) remains constant,

suggesting a growth control mechanism that is independent of cytoskeletal architecture. Future work may build on recent results that suggest that substrate stiffness potentiates unique myocytes physiological performance (Engler et al. 2008; Jacot et al. 2008). This is interesting work, because the substrate stiffness mimics the mechanical properties of the extracellular matrix in vivo. Thus, both the mechanical properties and geometric cues within the matrix possibly contribute to the shape, size, genetic profile, and physiological properties of muscle cells in the heart.

Acknowledgment We are grateful to the Harvard Center for Nano-scale Systems for use of their facilities.

Sources of Funding Harvard Materials Research Science and Engineering Center (MRSEC) sponsored by the National Science Foundation and the National Institutes of Health (1 R01 HL079126-01A2).

References

- Bray, M. A.; Sheehy, S. P.; Parker, K. K. Sarcomere alignment is regulated by myocyte shape. *Cell Motility Cytoskel.* 65(8): 641–651; 2008. doi:10.1002/cm.20290.
- Campbell, S. E.; Gerdes, A. M.; Smith, T. D. Comparison of regional differences in cardiac myocyte dimensions in rats, hamsters, and guinea pigs. *Anat. Rec.* 219(1): 53–59; 1987. doi:10.1002/ar.1092190110.
- Chen, C. S.; Mrksich, M.; Huang, S.; Whitesides, G. M.; Ingber, D. E. Geometric control of cell life and death. *Science.* 276: 1425–1428; 1997. doi:10.1126/science.276.5317.1425.
- Delbridge, L. M.; Satoh, H.; Yuan, W.; Bassani, J. W.; Qi, M.; Ginsburg, K. S.; Samarel, A. M.; Bers, D. M. Cardiac myocyte volume, Ca^{2+} fluxes, and sarcoplasmic reticulum loading in pressure-overload hypertrophy. *Am. J. Physiol-Heart Circ. Phys.* 272(5): 2425–2435; 1997.
- Engler, A. J.; Carag-Krieger, C.; Johnson, C. P.; Raab, M.; Tang, H. Y.; Speicher, D. W.; Sanger, J. W.; Sanger, J. M.; Discher, D. E. Embryonic cardiomyocytes beat best on a matrix with heart-like elasticity: scar-like rigidity inhibits beating. *J. Cell Sci.* 121(Pt 22): 3794–3802; 2008. doi:10.1242/jcs.029678.
- Gerdes, A. M. Cardiac myocyte remodeling in hypertrophy and progression to failure. *J. Card. Fail.* 8: S264–S268; 2002. doi:10.1054/jcaf.2002.129280.
- Gerdes, A. M.; Capasso, J. M. Structural remodeling and mechanical dysfunction of cardiac myocytes in heart failure. *J. Mol. Cell Cardiol.* 27: 849–856; 1995. doi:10.1016/0022-2828(95)90000-4.
- Glantz, S. A. Primer of Biostatistics. 5th ed. McGraw Hill, New York 2002.
- Huang, S.; Chen, C. S.; Ingber, D. E. Control of cyclin D1, p27(Kip1), and cell cycle progression in human capillary endothelial cells by cell shape and cytoskeletal tension. *Mol. Biol. Cell.* 9: 3179–3193; 1998.
- Jacot, J. G.; McCulloch, A. D.; Omens, J. H. Substrate stiffness affects the functional maturation of neonatal rat ventricular myocytes. *Biophys. J.* 95(7): 3479–3487; 2008. doi:10.1529/biophysj.107.124545.
- Lammerding, J.; Kamm, R. D.; Lee, R. T. Mechanotransduction in cardiac myocytes. *Ann. N.Y. Acad. Sci.* 1015: 53–70; 2004. doi:10.1196/annals.1302.005.

- LeDuc, P.; Bellin, R. Nanoscale intracellular organization and functional architecture mediating cellular behavior. *Ann. Biomed. Eng.* 34(1): 102–113. (12); 2006.
- Lindner, M.; Bohle, T.; Beuckelmann, D. J. Ca^{2+} -handling in heart failure—a review focusing on Ca^{2+} sparks. *Basic Res. Cardiol.* 97(Suppl 1): 179–182; 2002a. doi:10.1007/s003950200034.
- Lindner, M.; Brandt, M. C.; Sauer, H.; Hescheler, J.; Bohle, T.; Beuckelmann, D. J. Calcium sparks in human ventricular cardiomyocytes from patients with terminal heart failure. *Cell Calcium.* 31: 175–182; 2002b. doi:10.1054/ceca.2002.0272.
- Onodera, T.; Tamura, T.; Said, S.; McCune, S. A.; Gerdes, A. M. Maladaptive remodeling of cardiac myocyte shape begins long before failure in hypertension. *Hypertension.* 32: 753–757; 1998.
- Parker, K. K.; Brock, A. L.; Brangwynne, C.; Mannix, R. J.; Wang, N.; Ostuni, E.; Geisse, N. A.; Adams, J. C.; Whitesides, G. M.; Ingber, D. E. Directional control of lamellipodia extension by constraining cell shape and orienting cell tractional forces. *FASEB J.* 16: 1195–1204; 2002. doi:10.1096/fj.02-0038com.
- Parker, K. K.; Tan, J.; Chen, C. S.; Tung, L. Myofibrillar architecture in engineered cardiac myocytes. *Circ. Res.* 103: 340–342; 2008. doi:10.1161/CIRCRESAHA.108.182469.
- Tan, J. L.; Liu, W.; Nelson, C. M.; Raghavan, S.; Chen, C. S. Simple approach to micropattern cells on common culture substrates by tuning substrate wettability. *Tissue Eng.* 10: 865–872; 2004. doi:10.1089/1076327041348365.
- Walters, D. A.; Cleveland, J. P.; Thomson, N. H.; Hansma, P. K.; Wendman, M. A.; Gurley, G.; Elings, V. Short cantilevers for atomic force microscopy. *Rev. Sci. Instrum.* 67: 3583; 1996. doi:10.1063/1.1147177.
- Shorofsky, S. R.; Aggarwal, R.; Corretti, M.; Baffa, J. M.; Strum, J. M.; Al-Seikhan, B. A.; Kobayashi, Y. M.; Jones, L. R.; Wier, W. G.; Balke, C. W. Cellular mechanisms of altered contractility in the hypertrophied heart: big hearts, big sparks. *Circ. Res.* 84: 424–434; 1999.